CZECH TECHNICAL UNIVERSITY IN PRAGUE

Faculty of Nuclear Sciences and Physical Engineering

Department of Physics

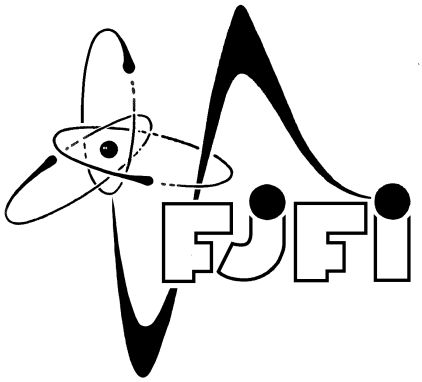

Simulation of cosmic ray showers for Pierre Auger Observatory

Research project

Prague, 2012 Elena Rakovská

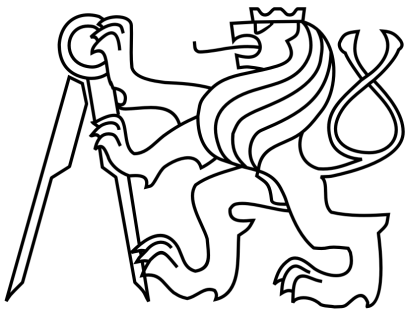

Declaration

Here I declare that I wrote my research project independently and exclusively with the use of cited bibliography.

I agree with usage of this thesis in accordance with the Act 121/2000 (Copyright Act).

Prague .....

.....
Elena Rakovská

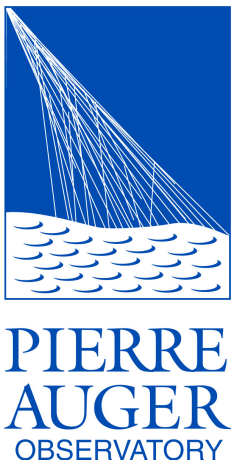

Acknowledgement

I am very grateful to my supervisor RNDr. Jiří Chudoba, Ph.D. and consultant RNDr. Petr Trávníček, Ph.D. for corrections and discussions about studied problematic. I would also like to thank to Dip. Phys. Colin Baus for technical support at the beginning of this research project.

Elena Rakovská

Title: **Simulation of cosmic ray showers for Pierre Auger Observatory**

Author: Elena Rakovská

Field of study: Nuclear Engineering

Specialization: Experimental nuclear physics

Type of work: Research project

Supervisor: RNDr. Jiří Chudoba, Ph.D., Institute of Physics AS CR

Consultant: RNDr. Petr Trávníček, Ph.D., Institute of Physics AS CR

Keywords: Pierre Auger Observatory, Air shower models, Shower universality, Muons, Missing energy

Abstract: Ultra High Energy Cosmic Rays (UHECR) represent the most energetic source of elementary particles available to scientists. They achieve macroscopic energies over 10^{20} eV from till now unidentified sources. The Toy model of shower development is described and demonstrated on simulations with CONEX. Part of the energy of primary particle is carried away by neutrinos and energetic muons. This particles are invisible for detector techniques of Pierre Auger Observatory and they create missing energy. The estimation of the missing energy is model dependent. The options for decreasing of this dependency are discussed in this work.

Contents

Introduction

This research project handles a topic of air shower simulations. It is divided into three main parts.

Very brief introduction into field of astroparticle physics is given in the first chapter. It is focused on the experiment Pierre Auger Observatory and questions connected with the highest energy cosmic rays.

The second chapter describes the toy model of shower development. Shower universality is demonstrated on the example of simulated showers. It explaines what function it has for analyzing of extensive air showers and what kind of differences could be observed in different shower components. Impact of interaction models dependence and mass composition is mentioned.

The third chapter concentrates on determination of missing energy at Pierre Auger Observatory. Estimation difficulties and improvements of this quantity are explained.

Chapter 1

Cosmic Rays in a Nutshell

In 2012 physicists are celebrating the 100th anniversary of the breaking balloon flight of Victor Hess from Czech republic to Germany. It was proofed for the first time that ionization of the air increases with altitude. It means the ionization is caused from particles coming from the universe. This event is considered as the "birth of comic rays" and Victor Hess received the Nobel price for the discovery in 1936. New point of understanding came later with Pierre Auger and his measurement of coincident events in different altitudes. An extensive air shower was observed and explained as particle cascade after interaction of very energetic primary particle in the atmosphere.

Cosmic rays were for many years the only source of high energy particles. For example the discovery of positron or muon was possible only due to cosmic rays. During the past years, it starts to dominate the strong advancement of man-made accelerators and the hunt for the maximum luminosity. But it will never be possible to reach few magnitude higher energies coming from the universe accelerators. Now the new era starts, the connection between precise data from LHC (Large Hadron Collider) and highest energy events from astroparticle experiments. Comparison of this two points of view is an unique opportunity for contemporary physics.

Diverse detection techniques were developed during past hundred years to investigate cosmic rays with different energies (pic. 1.1). There are many astroparticle experiments producing high quality data in whole range of energy spectrum, see pic. 1.2. There are some typical features of the flux of cosmic rays like knee, ankle and GZK cut-off.

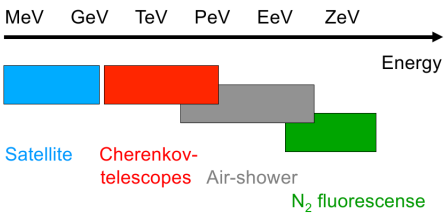

Figure 1.1: Detections techniques.

Although there is much known about the nature and composition of cosmic rays, it still produces many challenging questions for physics also nowadays. A motivation to investigate cosmic rays is actually still the same as hundred years ago. What kind of particles are flying from the universe to the Earth? Where are their sources and acceleration mechanism?

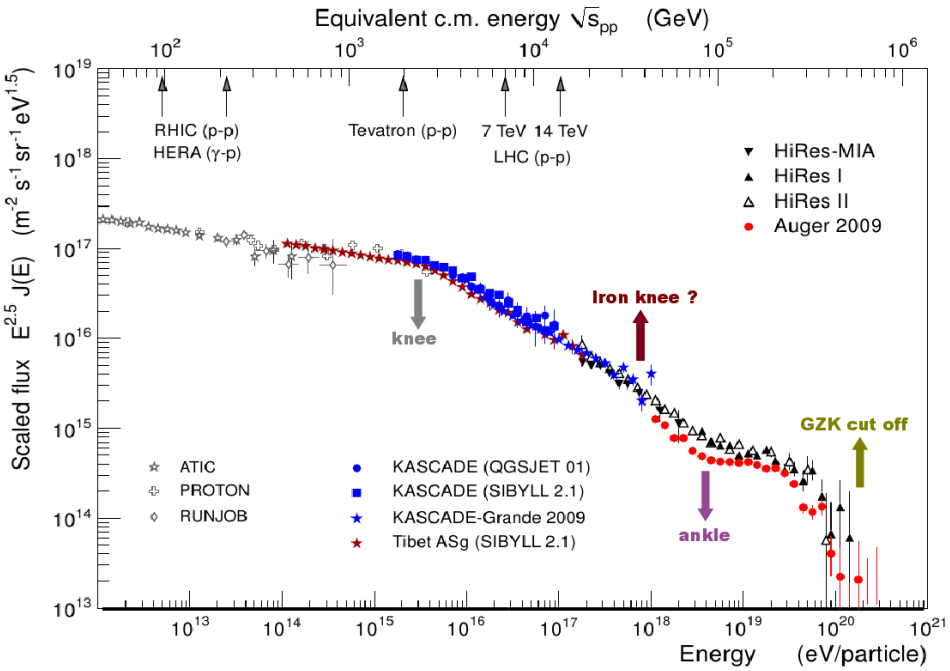

Figure 1.2: Cosmic rays spectrum without mass discrimination composed from different experiments, multiplied by $E^{2.5}$. On the upper axis is comparison to the collide experiments. Taken from [1].

1.1 Pierre Auger Observatory

Pierre Auger Observatory (PAO) is world leading experiment in the field of ultra high energy cosmic rays (UHECR). It covers the area of 3000 km^2 in Argentinean plain at altitude 1400 m a.s.l., see pic. 1.3. It started to collect data in 2004 and the collaboration consist of 17 countries. It is named after French physicist Pierre Auger and in fact it is trying to answer the same question, as he was asking many years ago: what kind of particles are hidden in cosmic rays, where are they coming from and how they reach their energies.

PAO uses as the first experiment hybrid detection techniques. The surface detector (principle based on Cherenkov light) includes 1600 water tanks with 1.5 km spacing. One of the detectors is shown in pic. 1.4. During clear moonless nights the surface measurement is supported by 24 fluorescence detectors (principle based on excitation of nitrogen molecules in the atmosphere) placed in four stations at the border of the field, one of them is shown in pic. 1.4. Next to the basic setup there are some upgrades and improvements making PAO sensitive to showers with energies down to 10^{17} eV. One of them is AMIGA (Auger Muons and Infill for the Ground Array) where is a denser grid on smaller area of water Cherenkov tanks together with underground muon detectors. There are also additional three telescopes HEAT (High Elevation Telescopes) with field of view above the basic ones. Another extension is AERA (Auger Engineering Radio Array) using radio detection principle to measure extensive air showers.

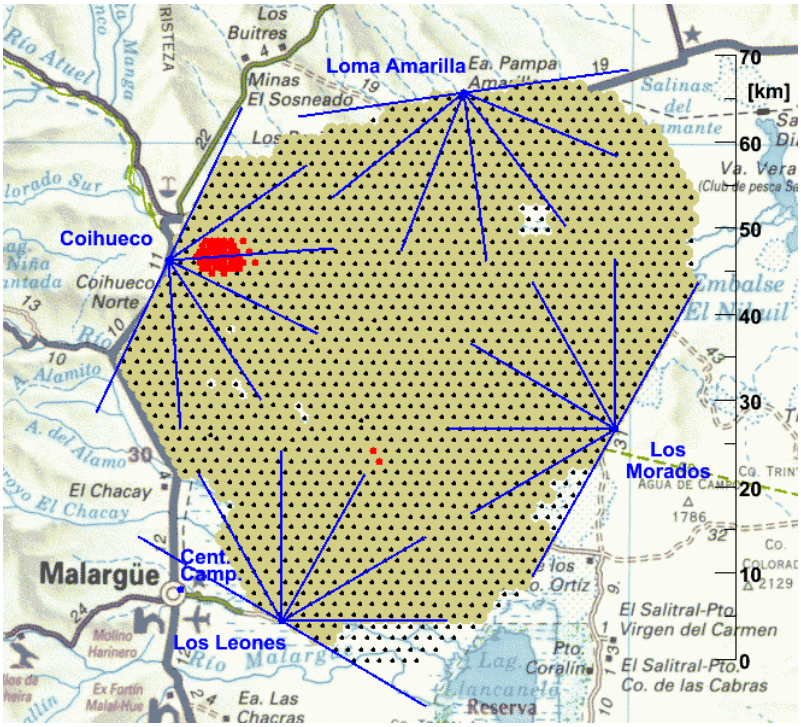

Figure 1.3: Detector layout of PAO near Argentinean city Malargue. Black dots are Cherenkov water tanks, blue lines show each of 24 optical telescopes. Red area shows AMIGA extension.

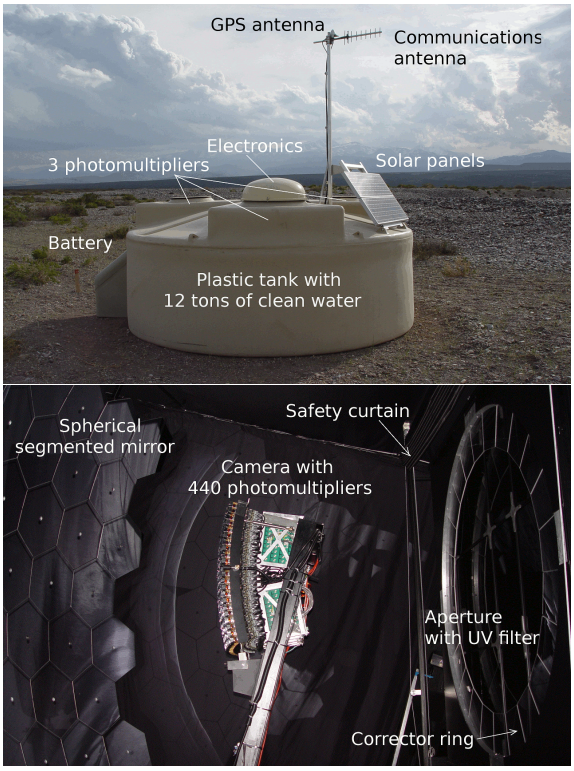

Figure 1.4: One surface detector (SD) on the top, detail of one fluorescence detector (FD) on the bottom.

Pierre Auger Observatory has currently very unique position among astroparticle physics experiments investigating UHECR. It has collected more data than any other experiment before and it is working in a hybrid mode. PAO latest results in energy spectrum agree with GZK cut-off prediction. Advances in mass composition determination (using X_{max}) show growing trend of the primary particle mass with energy, see pic. 1.5. Clear connection with particle physics is measurement of proton-air cross section at highest available energies (pic. 1.6) and σ^{inel}_{p-p} at $\sqrt{s} = 57$ TeV. The other important field of study at PAO is searching for sources of UHECR, which is connected with propagation of the particles, estimation of the extragalactic magnetic fields and astrophysical processes in the black holes.

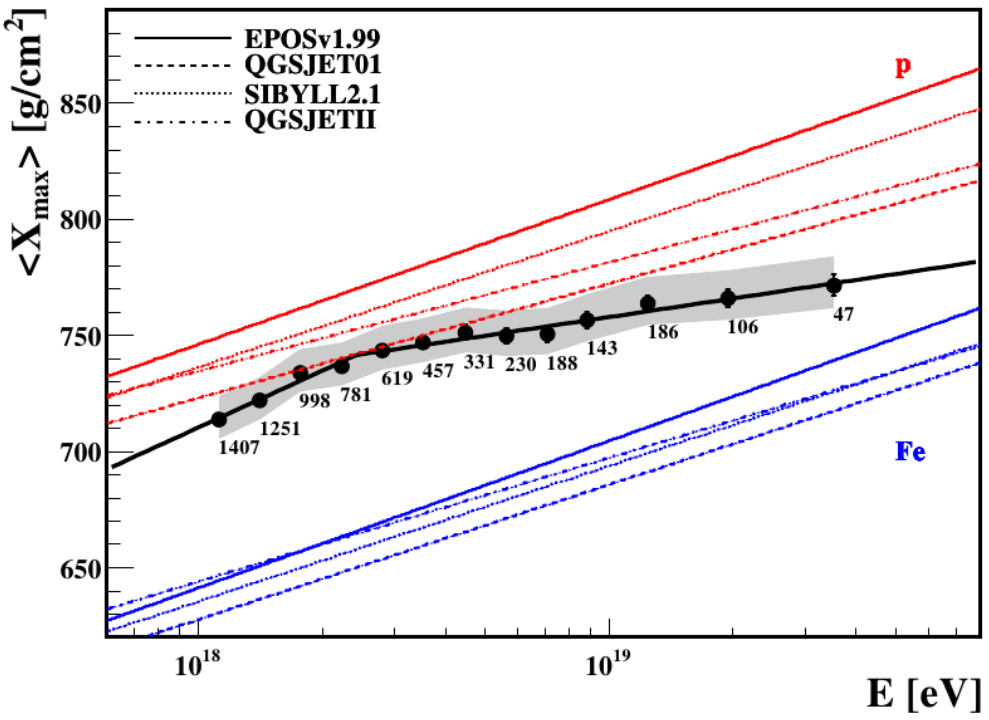

Figure 1.5: X_{max} as a function of the energy. Data (points) are compared with the model predictions for proton and iron primaries. The number of events in each bin is shown. Systematic uncertainties are indicated as a band. Taken from [2].

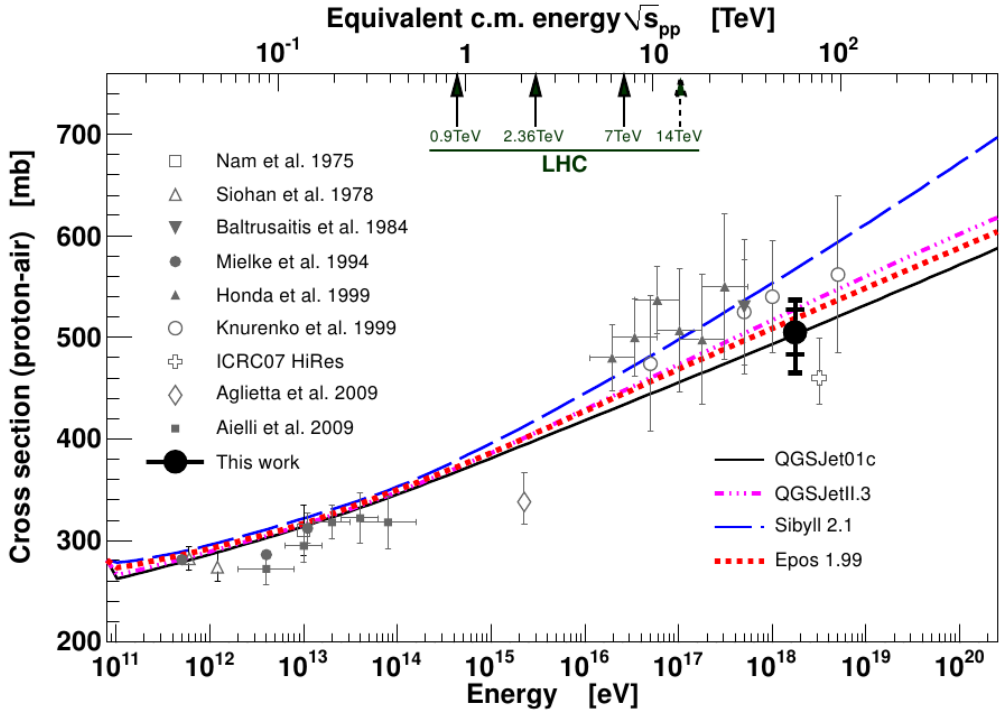

Figure 1.6: Proton air cross section calculated from PAO data and compared to various model predictions, from [3].

Chapter 2

Shower Universality

This chapter will discuss the topic of shower universality. What does it mean and how could it be used for analyzing extensive air showers? What kind of differences could be observed in electromagnetic and muon components? What does it say about mass composition?

Before introducing the idea of shower universality, it is necessary to understand main phenomena in shower development. Good approximation for description of this process is Toy model of extensive air showers.

2.1 Toy model of Air Shower development

The earth's atmosphere is in fact a large hadron calorimeter. A disadvantage could be that it is neither an usual sampling calorimeter with smart solution for light collection nor a classical homogeneous calorimeter, because the atmosphere's density varies with the altitude. From the other point of view, very positive attribute is the huge size. From the first interaction point the cascade starts to grow till X_{max} [g/cm^2], the atmospheric depth where the shower reaches maximum number of particles.

To imagine a development of extensive air shower, it is usual to divide it in three components: electromagnetic, hadronic and muons with neutrinos. There are two basics processes in the pure electromagnetic showers: bremsstrahlung and pair production. For the simplicity, there will be $e^{\pm}$ and γ replaced by universal particle of the same type a, see pic. 2.1.

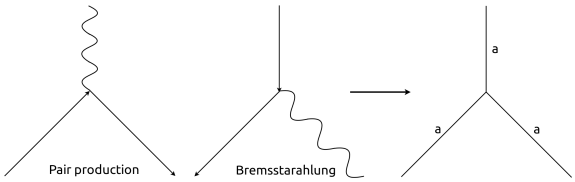

Figure 2.1: Simplified model of electromagnetic shower development.

It will be assumed that every particle decays (with electromagnetic interaction length λ) exactly in two particles with half energy of the mother particle. It means that in the zeroth generation there is just one particle with energy E_0, in the first generation are two particles with $E_0/2$,

second generation contains 4 particles with $E_0/4 = E_0/2^2$. Generally every particle in the n-th generation has energy $E_0/2^n$. The cascade follows this schema until particles have still enough energy for creating new particles. This energy is called critical energy, in the air $E_{crit} \approx 80$ MeV. When they jump below this threshold, competitive processes starts to be more important for energy looses, mainly ionization for $e^{\pm}$ and Compton scattering for γ. Maximum number of particles N_{max} occurs in the last generation n_{max} with energy E_{crit}. It means

$$N_{max} = 2^{n_{max}} = \frac{E_0}{E_{crit}} \Rightarrow n_{max} = \log_2\left(\frac{E_0}{E_{crit}}\right). \tag{2.1}$$

Shower maximum could be now obtained as

$$X_{max} = \lambda \cdot n_{max} = \lambda \cdot \log_2\left(\frac{E_0}{E_{crit}}\right). \tag{2.2}$$

To describe in similar way also hadronic component of the extensive air shower, it is useful to analyze expansion of the basic electromagnetic shower (Heitler's Model) from Matthews [4]. Lets consider a cascade caused by a single proton, see pic. 2.2.

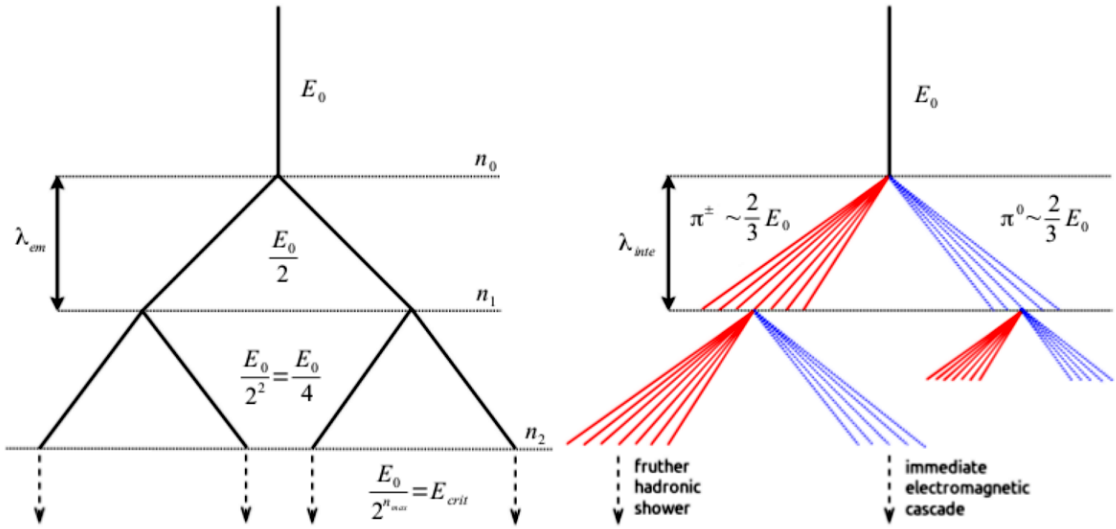

Figure 2.2: Electromagnetic shower development (on the left side) and its expansion to simplified model of hadronic shower cascade.

In inelastic processes there are equally produced mostly pions, as the lightest mesons. Energy of the primary particle is divided into $\frac{1}{3}$ to neutral pions, which immediately decay $\pi^0 \rightarrow 2\gamma$ and form later electromagnetic component. $\frac{2}{3}$ of E_0 are taken to charged pions $\pi^{\pm}$. Total number of particles is $N_{tot} = N_{\pi^0} + N_{ch}$ and energy in the n-th generation $E_n = \frac{E_0}{(N_{tot})^n}$. Analogically to electromagnetic shower, pions produce new generations until they have enough energy. We call this threshold E_{dec}, below that they decay. Charged pions follow mostly the process $\pi^{\pm} \rightarrow \mu^{\pm} + \overset{(-)}{\nu}_{\mu}$. Looking at the maximum of the shower, number of charged particles equals to number of muons,

$$N_{max(ch)} = N_{\mu} \Rightarrow \log N_{max(ch)} = \log N_{\mu} = n_{max} \cdot \log N_{max(ch)}. \tag{2.3}$$

Similarly as by the electromagnetic case, the n_{max} can be expressed as

$$\frac{E_0}{E_{dec}} = (N_{tot})^{n_{max}} \Rightarrow n_{max} = \frac{\log\left(\frac{E_0}{E_{dec}}\right)}{\log N_{tot}}. \tag{2.4}$$

Using this expression for the number of mouns

$$logN_\mu = \log\left(\frac{E_0}{E_{dec}}\right)^{\overbrace{\frac{\log N_{tot}}{\log N_{max(ch)}}}^{\alpha}} \Rightarrow N_{mu} = \left(\frac{E_0}{E_{dec}}\right)^{\alpha}. \tag{2.5}$$

At the highest energies, there are expected mainly hadronic primaries like proton, α particles and iron nuclei. Considering heavy nuclei as primary with A number of nucleons, the energy E_0 divides equally into each nucleon $E_{nuc} = \frac{E_0}{A}$. Superposition principle allows to imagine shower caused by heavier nuclei as a sum of A individual proton showers with initial energy E_{nuc}, see pic.2.3.

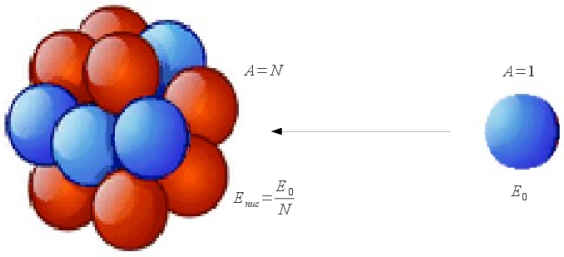

Figure 2.3: Superposition principle.

It is interesting to look how the shower maximum vary with different kind of primary particles. In the relation 2.2 it will be replaced interaction length with elongation rate D_e [g/cm^2] which counts with changing of λ in different altitudes and also $\log_2$ by ln,

$$X_{max} = D_e \cdot \ln\left(\frac{E_0}{E_{crit}}\right) \overset{A\geq 1}{=} D_e \cdot \ln\left(\frac{E_0/A}{E_{crit}}\right) = D_e\left(\ln\frac{E_0}{E_{crit}} - \ln A\right). \tag{2.6}$$

It means, that a mass sensitive parameter is hidden in elongation rate inside of X_{max}, because

$$X^A_{max} = X^p_{max} - D_e \cdot \ln A. \tag{2.7}$$

Similarly from the superposition point of view, it is obvious that the number of particles in maximum is equal for all showers with the same initial energy of nuclei,

$$N^A_{max} = A \cdot \frac{E_0/A}{E_{eff}} = \frac{E_0}{E_{eff}} = N^p_{max}, \tag{2.8}$$

where the E_{eff} takes into account E_{crit} and also E_{dec}. For number of muons it is possible to receive analogical relation to 2.5 for heavier nuclei primaries,

$$N^A_\mu = A \cdot \left(\frac{E_0/A}{E_{dec}}\right)^{\alpha} = A^{1-\alpha}\left(\frac{E_0}{E_{dec}}\right)^{\alpha} = A^{1-\alpha} \cdot N^p_\mu. \tag{2.9}$$

Number of muons becomes another important mass sensitive parameter.

2.2 CONEX

Conex [5],[6],[7] is a combination of Monte Carlo simulation of high energy interactions and fast numerical solution of cascade equations. It is designed for quick one-dimensional simulation of shower profiles, including energy deposit, charged particles and muon longitudinal profiles. This program was used for simulation in this section. For shower generation were most used hadron interaction models QGSJet II, EPOS, Sybill.

The conclusion about total number of charged particles and muons for proton, iron and gamma showers, which was calculated above, is demonstrated on the pic. 2.4. Results were simulated with EPOS hadronic model for different primaries. For each type of shower, it was generated 1000 showers with energy of primary particle in range $10^{19} - 10^{21}$ eV and zenith angle between 0°and 60°. Similar graphs were obtained also with other models. The same was calculated also for primaries with lower energies between $10^{17} - 10^{19}$ eV on the pic. 2.5.

To see explicitly differences in single model predictions, it was compared iron and proton showers separately. Number of muons and charged particles in showers caused by iron in energy range $10^{19} - 10^{21}$ eV with different models is on the pic. 2.6, for lower energies $10^{17} - 10^{19}$ eV on the pic. 2.7. The same situation for protons is projected in pic. 2.8 and pic. 2.9.

The idea of shower universality is based on concept that air cascade in maximum does not grow any more. From this point the shower follows rules of electromagnetism, which are very well understood. It is not important, how exactly or how fast the shower reaches its maximum. It means that for equally energetic showers observed in the same point of their development ($X - X_{max}$), the electromagnetic component has the same size for all primary particles. Using this concept it could be significantly reduced also differences between models. The same concept does not hold for number of muons, which is strong correlated with type of primary particle. Simulated results are shown for higher energies on pic. 2.12 and 2.10, for lower energies on pic. 2.13 and 2.11. The error bars on this plots represent RMS of the distributions of the displayed quantities. To see easier differences between iron and proton showers, on the pic. 2.14 and 2.15 are plotted the ratios of N(Fe)/N(p) and Mu(Fe)/Mu(p). Differences in number of muons between interaction models are obvious on the pic. 2.16 for higher energies and pic. 2.17 for lower energies.

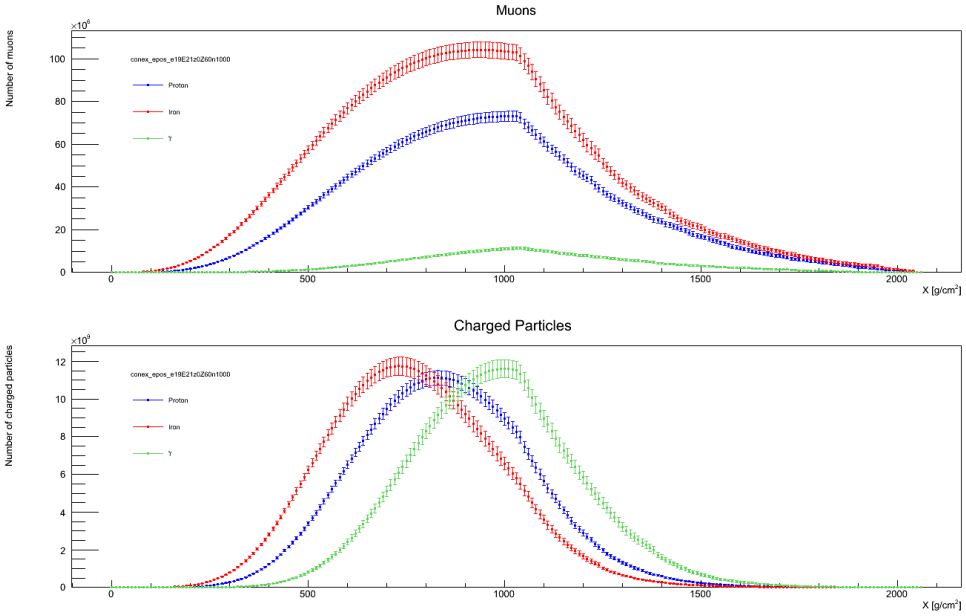

Figure 2.4: Number of muons (up) and charged particles (down) depending on atmospheric depth X for three shower types with primary energies $10^{19} - 10^{21}$ eV.

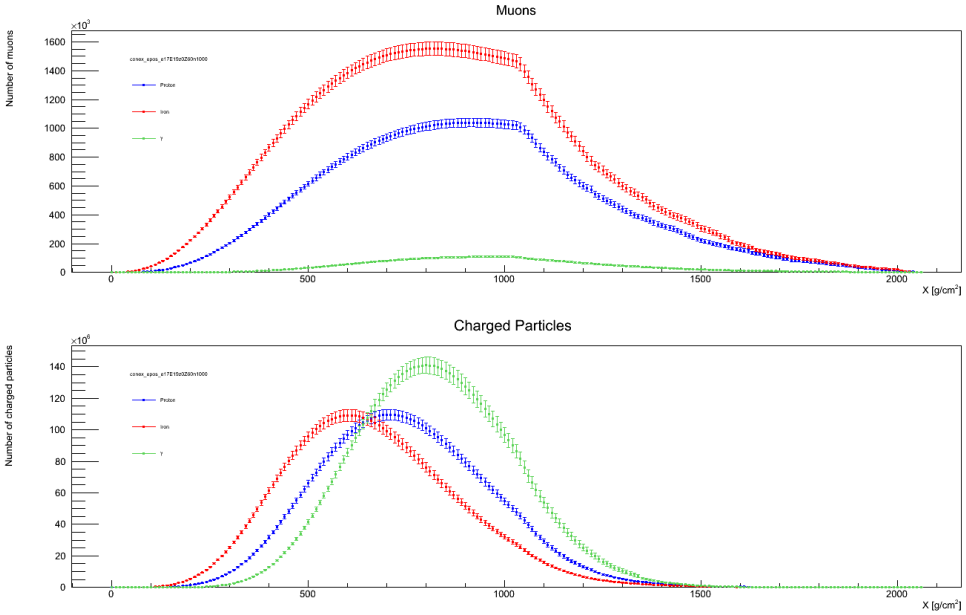

Figure 2.5: Number of muons(up) and charged particles (down) depending on atmospheric depth X for three shower types with primary energies $10^{17} - 10^{19}$ eV.

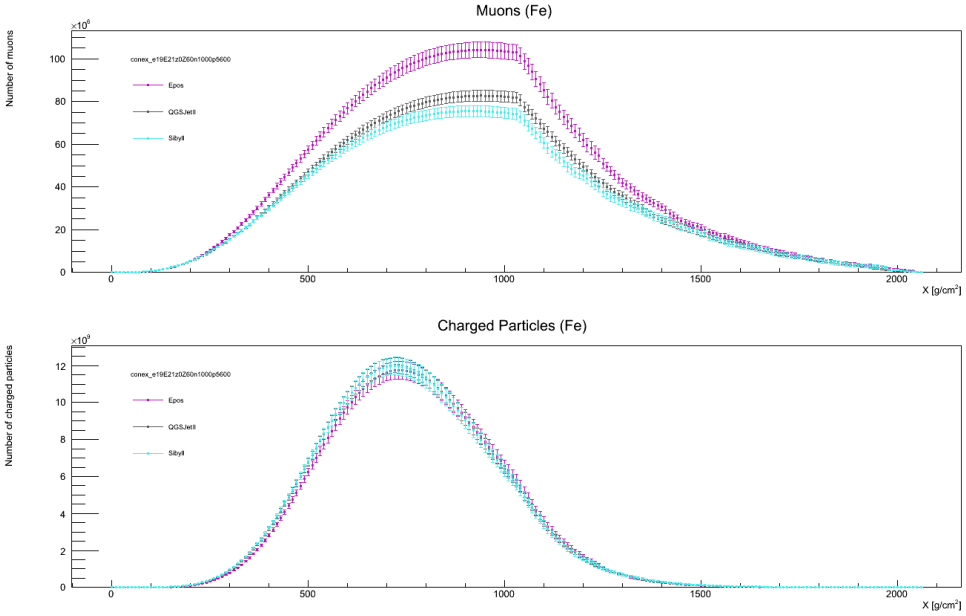

Figure 2.6: Number of muons(up) and charged particles (down) depending on atmospheric depth X from iron showers for three models and energies $10^{19} - 10^{21}$ eV.

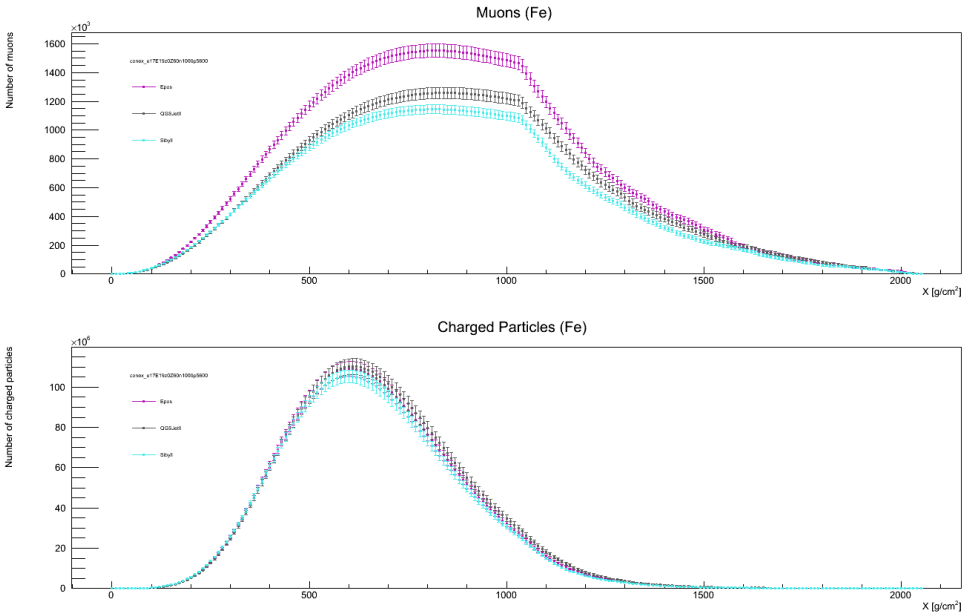

Figure 2.7: Number of muons(up) and charged particles (down) depending on atmospheric depth X from iron showers for three models and energies $10^{17} - 10^{19}$ eV.

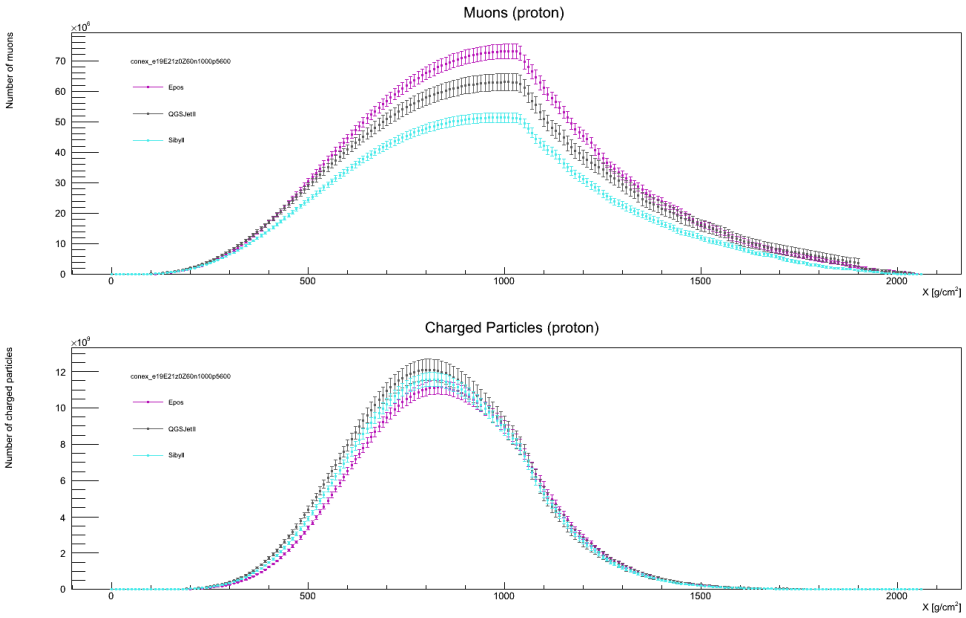

Figure 2.8: Number of muons(up) and charged particles (down) depending on atmospheric depth X from proton showers for three models and energies $10^{19} - 10^{21}$ eV.

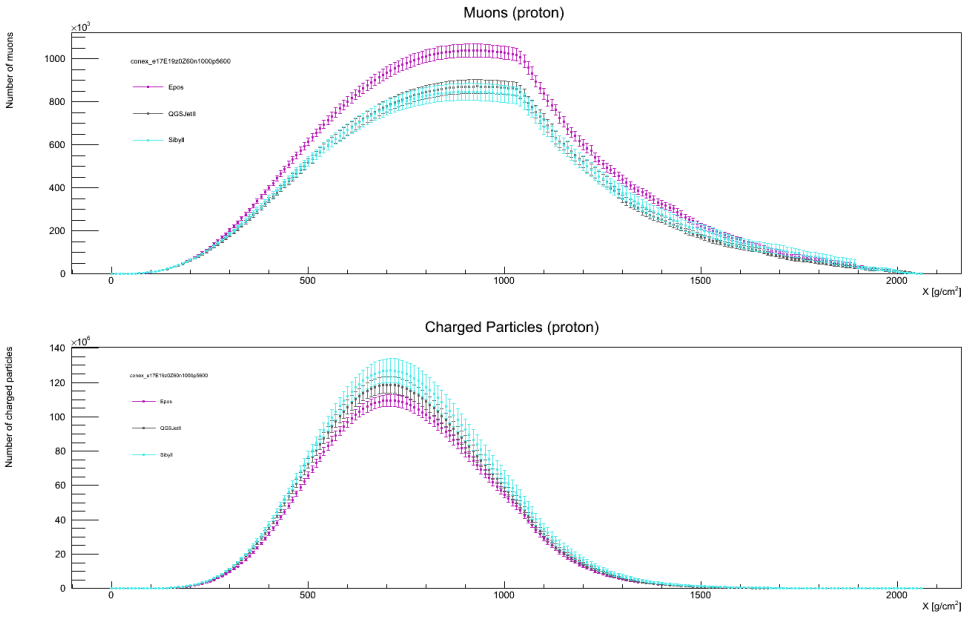

Figure 2.9: Number of muons(up) and charged particles (down) depending on atmospheric depth X from proton showers for three models and energies $10^{17} - 10^{19}$ eV.

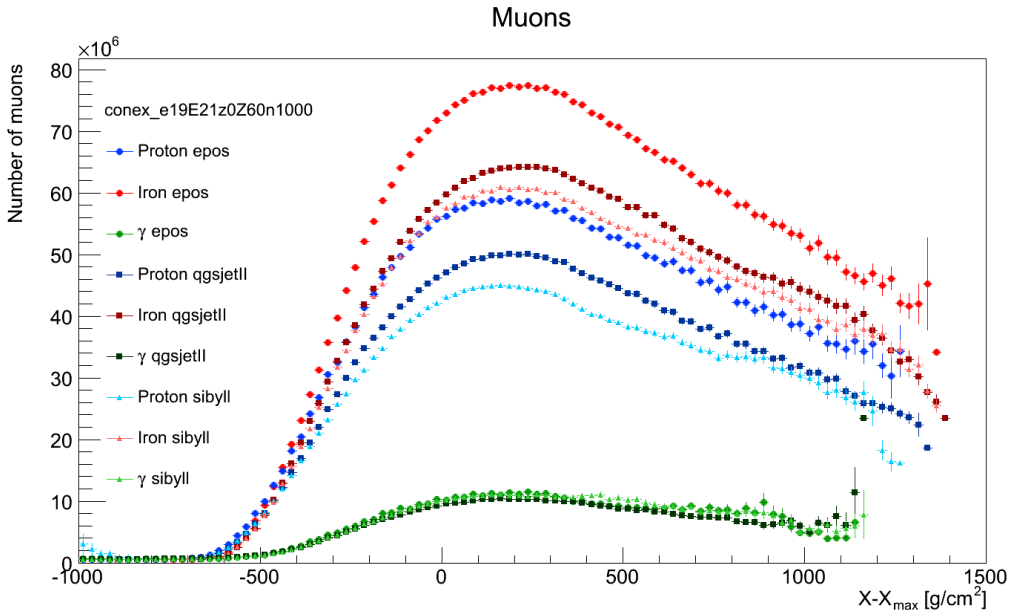

Figure 2.10: Number of muons in dependence to $X - X_{max}$ for proton, iron and γ showers using three models with energies $10^{19} - 10^{21}$ eV.

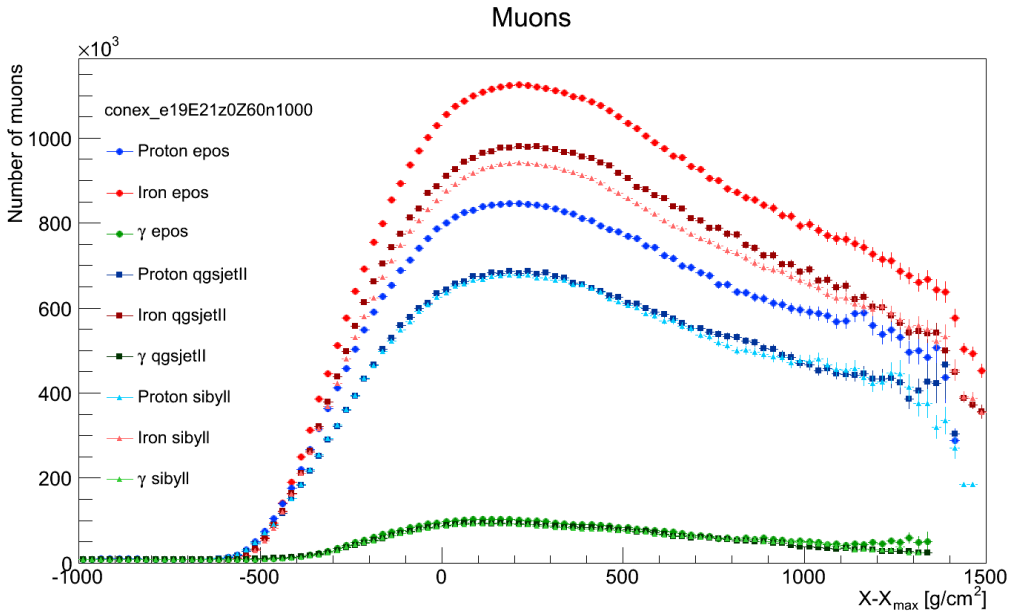

Figure 2.11: Number of muons in dependence to $X - X_{max}$ for proton, iron and γ showers using three models with energies $10^{17} - 10^{19}$ eV.

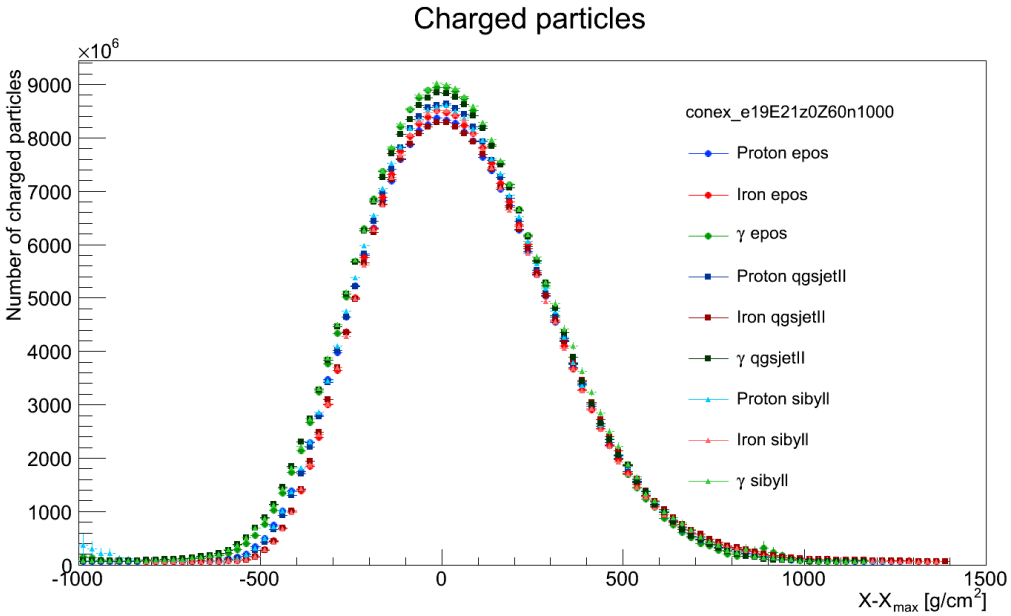

Figure 2.12: Number of charged particles in dependence to $X - X_{max}$ for proton, iron and γ showers using three models with energies $10^{19} - 10^{21}$ eV.

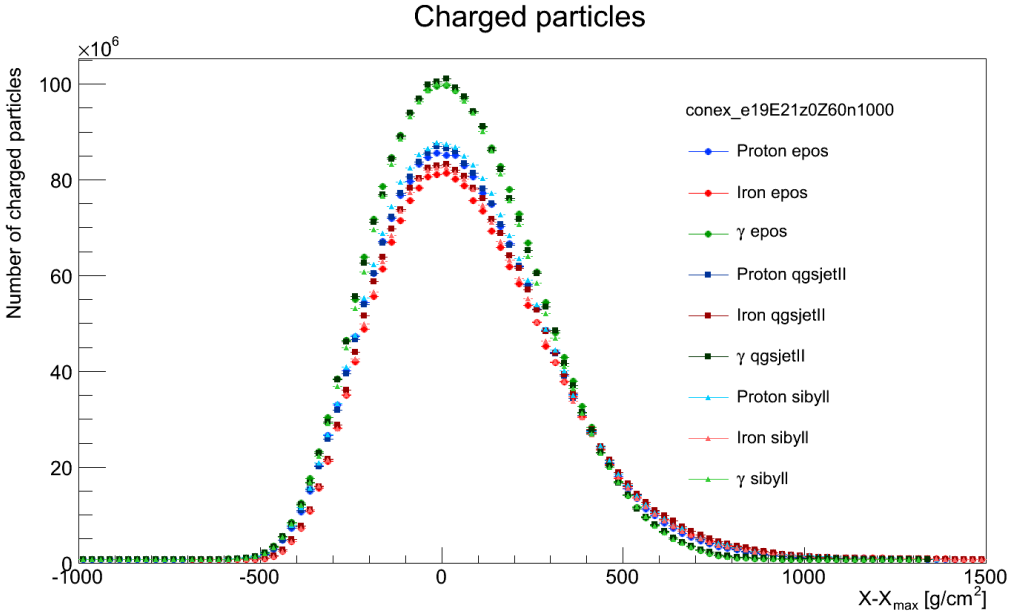

Figure 2.13: Number of charged particles in dependence to $X - X_{max}$ for proton, iron and γ showers using three models with energies $10^{17} - 10^{19}$ eV.

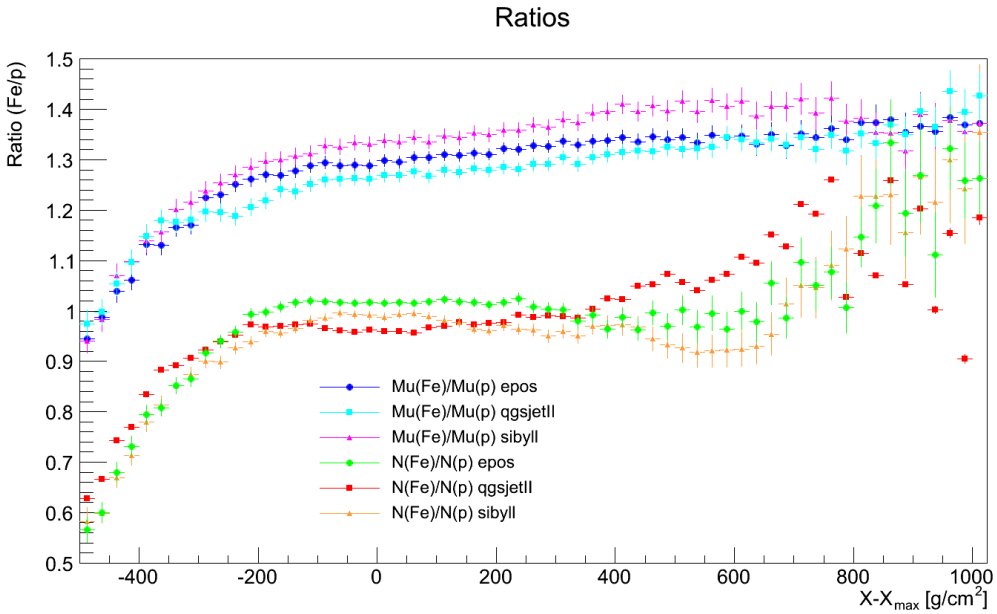

Figure 2.14: Ratio of muons and charged particles between iron and proton showers using three models with energies $10^{19} - 10^{21}$ eV.

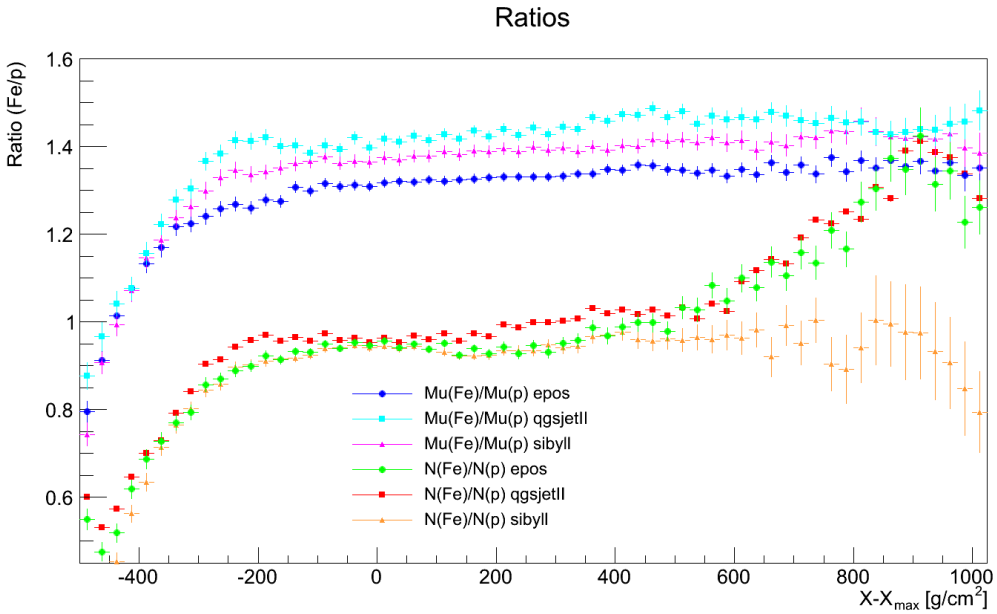

Figure 2.15: Ratio of muons and charged particles between iron and proton showers using three models with energies $10^{17} - 10^{19}$ eV.

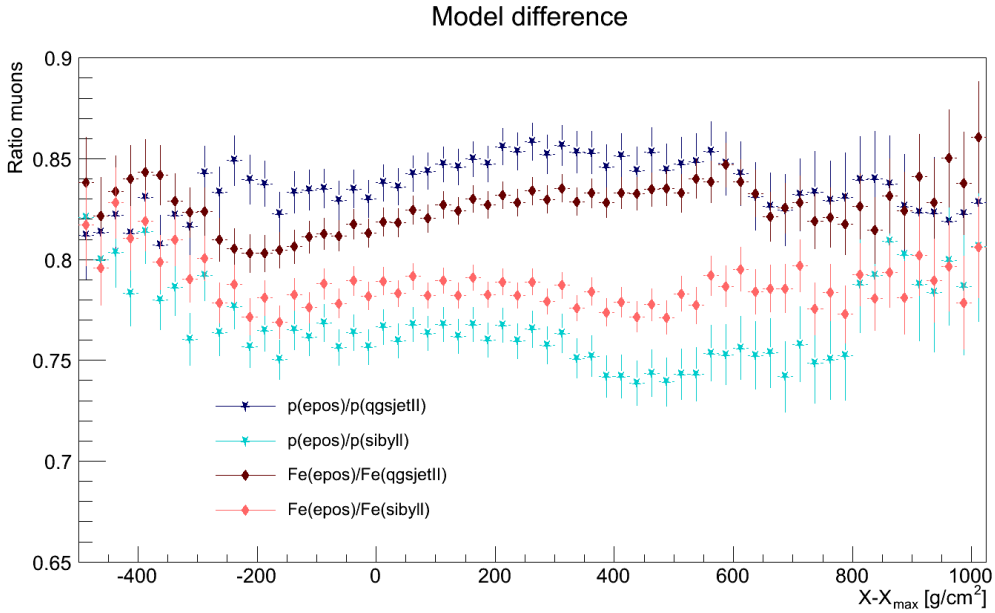

Figure 2.16: Number of muons from proton and iron showers obtained from Epos model in ratio with the same quantity from QGSJet II and Sibyll models, energy range $10^{19} - 10^{21}$ eV.

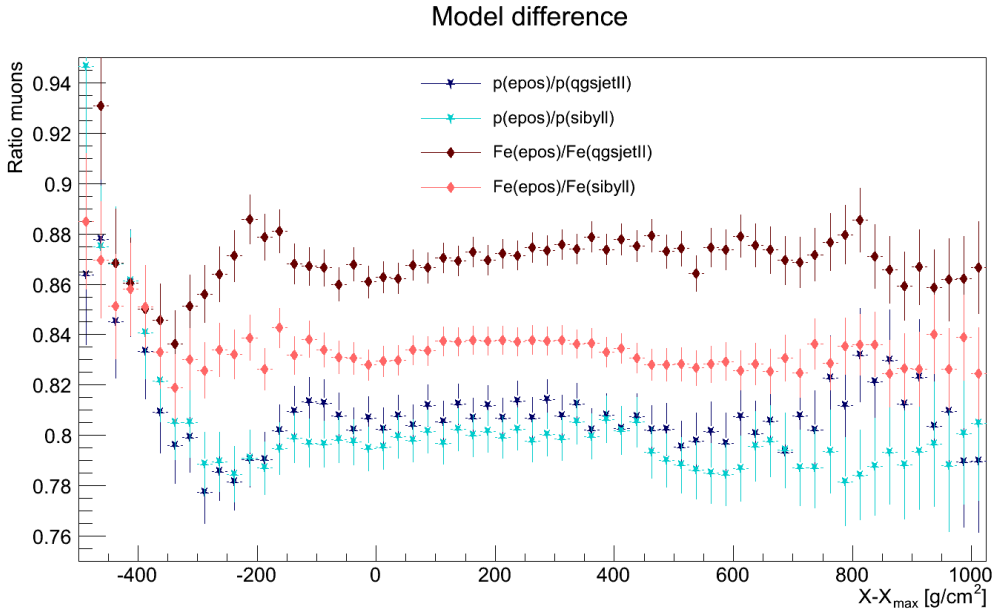

Figure 2.17: Number of muons from proton and iron showers obtained from Epos model in ratio with the same quantity from QGSJet II and Sibyll models, energy range $10^{17} - 10^{19}$ eV.

Chapter 3

Missing energy

This chapter explains closer problematics of missing energy and how the universality of the air shower could be used for energy calibration and determination of the missing energy. What are the differences considering this parameters between regular and Infill array at Pierre Auger Observatory?

3.1 Muon impact on missing energy

The shower profiles from the fluorescence light are measured with telescopes. The parametrization of the profile dE/dX is done with Gaisser-Hillas function [8]

$$f_{GH}(X) = \frac{dE}{dX}(X_{max}) \left(\frac{X - X_0}{X_{max} - X_0} \right)^{\frac{X_{max}-X_0}{\lambda}} e^{\frac{X_{max}-X}{\lambda}}. \tag{3.1}$$

The energy reconstruction of the primary particle E_0 could be obtained simply by integration of the profile, it is so called calorimetric energy

$$E_{cal} = \int_0^\infty f_{GH}(X) dX. \tag{3.2}$$

Part of the energy is by shower development carried away by neutrinos and energetic muons. This particles are invisible for detector techniques of Pierre Auger Observatory and are described as missing energy E_{miss}. Energy of the primary particle is estimated as $E_0 = E_{cal} + E_{miss}$. The missing energy is usually obtained from Monte-Carlo simulation. Because the exact mass composition is unknown and non of the interaction models could be preferred, E_{miss} is determined as average of all models for mixed composition. The spread between model predictions for different primaries is notable (see pic.3.1).

Using the correlation of energetic muons on the ground with missing energy, it is possible significantly reduce the error by E_{miss} estimation [10]. Because energy deposit of muons is small, they are not measured by fluorescence detector and they contribute from large part to missing energy. Many of energetic muons reach the ground and bring direct information about the amount of E_{miss}, see pic. 3.2. This

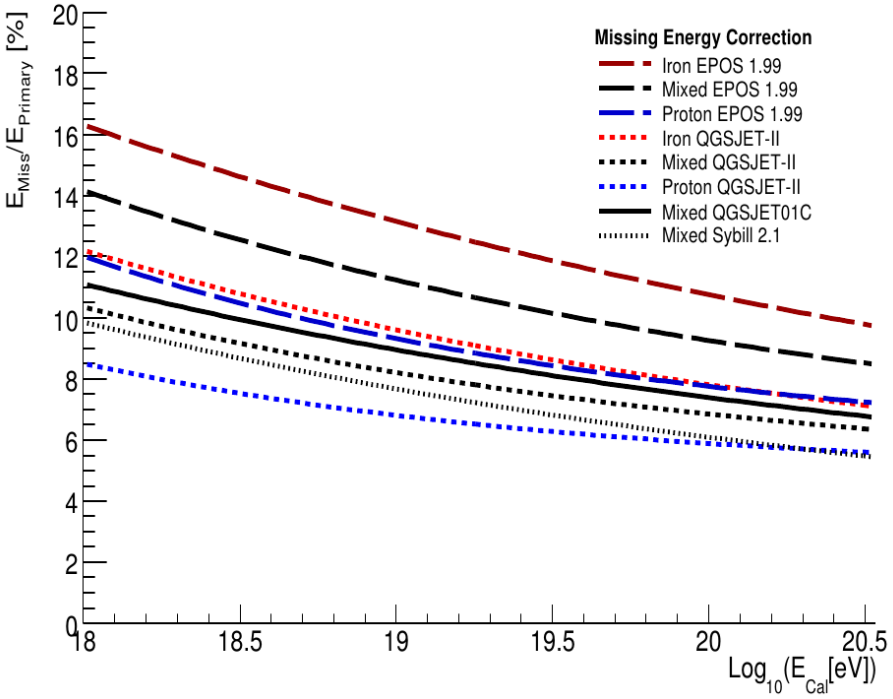

Figure 3.1: Missing energy for different primaries with most used interaction models in percent of primary particle energy. In this text $E_0 = E_{Primary}$. Taken from [9].

parametrization decreases the dependence on interaction models and also on type of primary particle. With new extension AMIGA at Pierre Auger Observatory, it will be feasible to obtain better data about amount of muons on the ground. E_{miss} must not be added as universal value but it could be counted shower-by-shower.

Very simply by using Heitler-Matthews model (discussed in second chapter) primary energy can be expressed [9]

$$E_0 = \xi_{ecrit} N_{max} + \xi_{\pi crit} N_\mu \approx \xi_{ecrit} N_{max} + E_{miss}, \tag{3.3}$$

where ξ_{crit} is critical energy for electromagnetic particles resp. pions. This basic approximation is in agreement with the results mentioned above (linear correlation between N_μ and E_{miss}). Taking advantage of hybrid detection at Pierre Auger Observatory, there are two well measured values: from SD signal at 1000 m from the shower core $S(1000)$ and from FD the atmospheric slant depth of shower maximum X_{max}. Using shower universality, $S(1000)$ could be related to N_μ when cascades are compared in the same stage of development ($X_{max} - X_{ground}$). Applying simplified "Toy model of missing energy", it is possible to express missing energy as function $E_{miss}(S(1000), X_{max} - X_{ground})$. Dependence on models and mass composition is also significantly reduced, see pic. 3.3.

3.2 Infill Array

With Pierre Auger upgrade on Surface Array it is possible to detect air showers with energy down to 10^{17} eV [11]. The extension consist of three high elevation

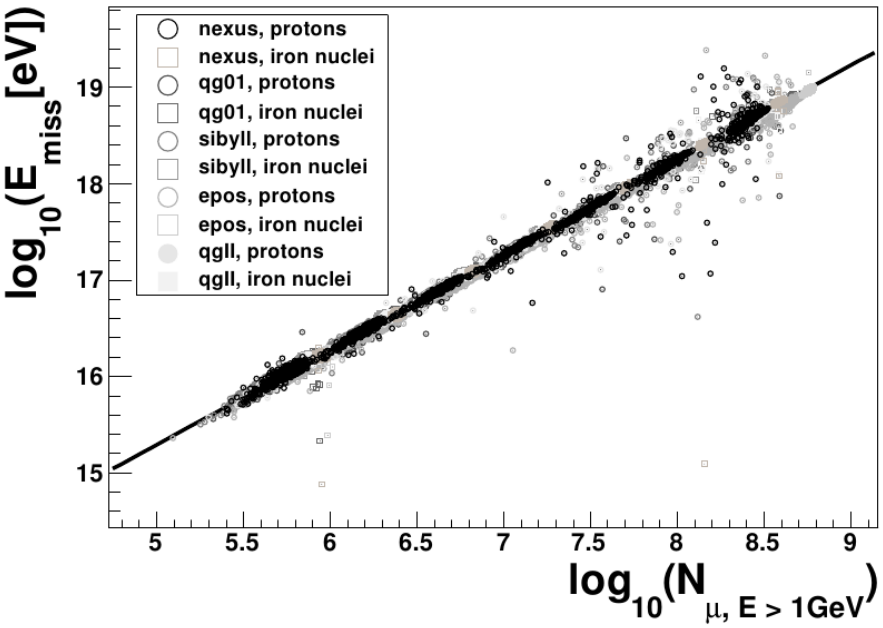

Figure 3.2: Correlation between muons with $E_\mu > 1$ GeV and size of missing energy for vertical showers (zenith angle $\Theta = 0°$). Black line is fitted parametrization function. Taken from [10].

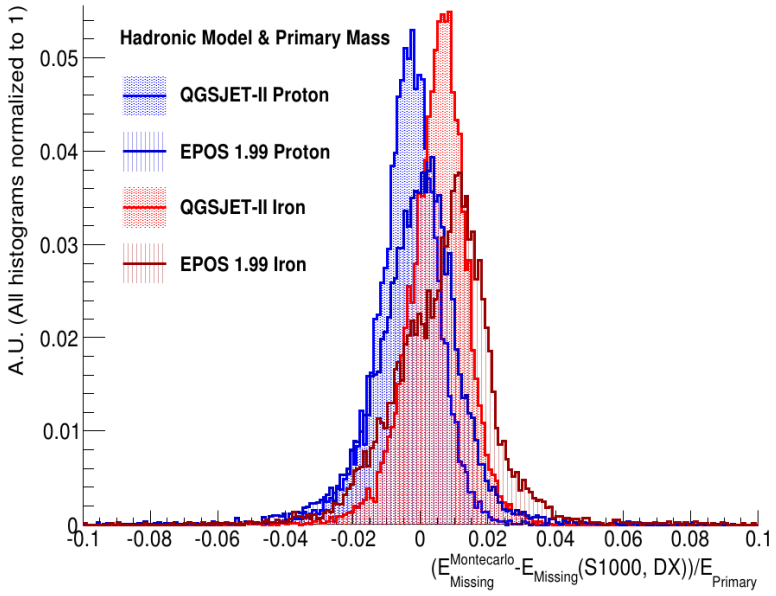

Figure 3.3: Difference between estimation of missing energy $E_{miss}(S(1000), X_{max} - X_{ground})$ and Monte-Carlo based method in units of primary energy. Taken from [9].

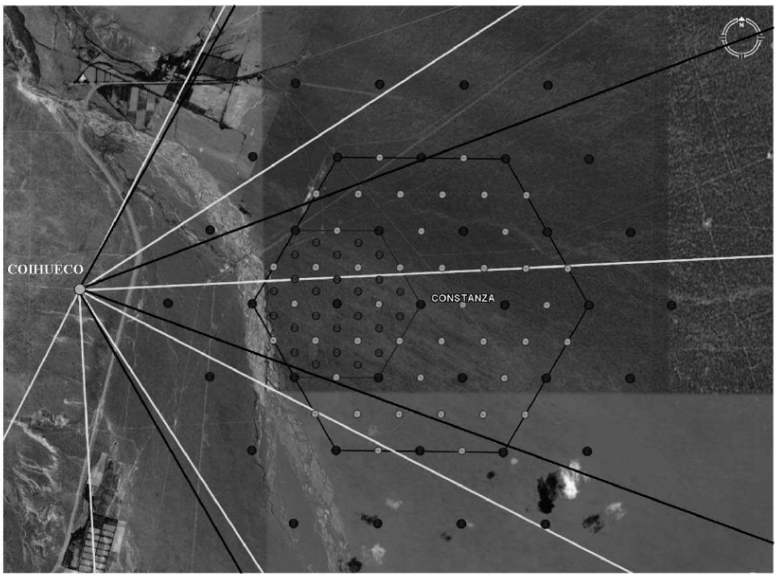

Figure 3.4: Layout of AMIGA extension. White and black lines show the six original and three enhanced telescopes. Grey, white and black dots indicate surface detectors plus buried muon counters placed 433, 750, and 1500 m apart. Taken from [11].

telescopes (HEAT) and an infilled area (23.5 from 3000 km^2) with additional 85 pair of Cherenkov surface detectors and underground muon scintillator counters covering area of 30 m^2(AMIGA). The enhancement is placed 6 km away from Coihueco station, see pic. 3.4

Missing energy increases with lower energies, that why the estimation of E_{miss} for Infill Array is of high interest. The combination of both methods, mentioned above, could be an interesting topic to explore.

Conclusion

After the introduction in the first chapter about astroparticle physics and biggest experiment in this field, the project was focused on air showers and their simulations.

The Toy model of development of electromagnetic showers and its extension to hadronic showers was discussed in details. Conclusions were demonstrated on air shower simulations. Topic of the second chapter was shower universality and differences in single components of shower cascades. Hadron interaction models and mass composition dependence was shown on simulations.

The third chapter was concentrated on missing energy, where it was explained the importance and difficulties of its estimation. On the example of Pierre Auger Observatory, improvements in the method of calculation of missing energy was discussed. The topic for further research was mentioned.

Bibliography

[1] D. dEnterria, R. Engel, T. Pierog, S. Ostapchenko, and K. Werner. Constraints from the first lhc data on hadronic event generators for ultra-high energy cosmic-ray physics. *Astroparticle Physics*, 35(2):98–113, 2011.

[2] P.F. San Luis. The distribution of shower maxima of uhecr air showers. *Proc. 32nd ICRC, Beijing, China*, 2011.

[3] R. ULRICH. Estimate of the proton-air cross-section with the pierre auger observatory. *Proc. 32nd ICRC, Beijing, China*, 2011.

[4] J. Matthews. A heitler model of extensive air showers. *Astroparticle Physics*, 22(5):387–397, 2005.

[5] T. Bergmann et al. One-dimensional hybrid approach to extensive air shower simulation. *Astropart. Phys.*, 26:420–432, 2007.

[6] T. Pierog et al. First results of fast one-dimensional hybrid simulation of eas using conex. *Nucl. Phys. Proc. Suppl.*, 151:159–162, 2006.

[7] G. Bossard et al. Cosmic ray air shower characteristics in the framework of the parton-based gribov-regge model nexus. *Phys. Rev.*, D63:054030, 2001.

[8] TK Gaisser and AM Hillas. Reliability of the method of constant intensity cuts for reconstructing the average development of vertical showers. In *International Cosmic Ray Conference*, volume 8, pages 353–357, 1977.

[9] A.G. for The Pierre Auger Collaboriation Mariazzi. A new method for determining the primary energy from the calorimetric energy of showers observed in hybrid mode on a shower-by-shower basis. *Arxiv preprint arXiv:1107.4804*, ICRC Beijing 2011.

[10] M. Nyklíček and P. Trávníček. On the size of missing energy of cosmic ray showers. *icrc2009.uni.lodz.pl/proc/pdf/icrc0240.pdf*, ICRC Lodz 2009.

[11] A. Etchegoyen and Collaboration Pierre Auger. Amiga, auger muons and infill for the ground array. *Arxiv preprint arXiv:0710.1646*, 2007.